



**HAL**  
open science

## A new way to analyse the size effect in quasi-brittle materials by scaling the heterogeneity size

Syed Yasir Alam, Ran Zhu, Ahmed Loukili

► **To cite this version:**

Syed Yasir Alam, Ran Zhu, Ahmed Loukili. A new way to analyse the size effect in quasi-brittle materials by scaling the heterogeneity size. *Engineering Fracture Mechanics*, 2020, 225, pp.106864 -. 10.1016/j.engfracmech.2019.106864 . hal-03489516

**HAL Id: hal-03489516**

**<https://hal.science/hal-03489516>**

Submitted on 7 Mar 2022

**HAL** is a multi-disciplinary open access archive for the deposit and dissemination of scientific research documents, whether they are published or not. The documents may come from teaching and research institutions in France or abroad, or from public or private research centers.

L'archive ouverte pluridisciplinaire **HAL**, est destinée au dépôt et à la diffusion de documents scientifiques de niveau recherche, publiés ou non, émanant des établissements d'enseignement et de recherche français ou étrangers, des laboratoires publics ou privés.



Distributed under a Creative Commons Attribution - NonCommercial 4.0 International License

# A new way to analyse the size effect in quasi-brittle materials by scaling the heterogeneity size

Syed Yasir Alam, Ran Zhu, Ahmed Loukili

Institut de Recherche en Génie Civil et Mécanique (GeM), UMR-CNRS 6183,  
Ecole Centrale de Nantes, France.

**Abstract:** Size effect has been a major problem in the design of quasi-brittle materials like concrete. The existing approaches consider the determination of size independent properties mainly by testing geometrically similar specimens. These specimens vary in size from small to large. Often it is difficult to perform testing on these specimens because of their size. Moreover, these approaches do not consider the role of microstructure or the heterogeneity size, which is the source of size effect. In this paper, a new size effect model is presented, which takes into account the heterogeneity size (aggregate size for concrete). Several series of tests are performed on concrete where an original approach to investigate size effect is applied by scaling the heterogeneity size instead of scaling the specimen size. The proposed size effect model makes it possible to determine the size independent fracture properties. The role of the ratio of the structural size to the heterogeneity size is clearly established in the size effect approach. The size effect curve and the fracture parameters obtained by using new size effect model perfectly match with those of Bažant's size effect; however, the former is much easier to perform experimentally or numerically.

**Keywords:** concrete, aggregate size, size effect, fracture energy, heterogeneity size

## 1. Introduction

The nominal strength leading to brittle failure of structures made with quasi-brittle materials like concrete generally exhibits a significant size effect. In general, as a good design principle, the failure should occur after large stable crack growth. Here the size effect is caused by the global release of stored energy during large fracture and is generally termed as Type II size effect. It is firmly established that the size effect of quasi-brittle materials such as concrete, mortar, rocks or wood is an energetic size effect and not a statistical one in the sense of the Weibull's statistics ([Weibull 1939](#)).

It is typically accepted that during the failure of quasi-brittle materials such as concrete, coarse grained ceramics and fibre-reinforced composites, the development of a fracture process zone (FPZ) leads to a stable crack growth prior to the attainment of peak load ([Alam et al. 2014](#)). This sizeable FPZ is physically considered as the source of size effect and regarded as an intrinsic property of quasi-brittle materials. The occurrence of the FPZ is directly attributed to heterogeneity of the material microstructure. The cementitious materials are highly heterogeneous by design and the heterogeneity size varies as the length scale varies. At the scale of concrete structures, material heterogeneity is caused by the presence of coarse aggregates. However, at the scale of mortar, material heterogeneity is caused by the presence of sand particles. Going further down, at the scale of cement paste, the hydration products, cement clinker and pores play the role of heterogeneities. Furthermore, at the nanometric scale, the material becomes more complex and can be considered as an agglomerate of various molecules. These heterogeneities may have an important role on the

behaviour of material and must be considered in the size effect problem. Taking concrete as an example, size effect is significantly affected by the size of heterogeneities (aggregate particles). Significant amount of literature has investigated the effect of aggregate size on the fracture process zone. However, its relationship with size effect problem is not yet understood.

Aggregate accounts for almost 60%-80% of the volume and 70%-85% of the weight of concrete of which, coarse aggregate occupies about 45 % of the volume of concrete (Neville 2011). Coarse aggregate properties, such as grading, surface area, particle size and shape, angularity, surface texture, mineralogy, water absorption and strength have been investigated (Aïtcin et al. 1990; Goble and Cohen 1999; Wu et al. 2001). Among these properties, maximum aggregate size ( $d_{max}$ ) is considered as one of the important parameters that affect the properties of the hardened concrete. The effect of  $d_{max}$  on the mechanical properties of concrete is a complex problem. It is generally considered that the coarse aggregates affect the crack propagation by crack bridging and microcrack shielding, which cause the reduction of stress in the fracture zone. Also, the interlocking of the particles between the crack surfaces consumes energy and thus enhances the fracture resistance, leading to the improvement of concrete strength (Wu et al. 2001).

Apart from the influence on mechanical properties of concrete, aggregate size also has an impact on the fracture parameters and brittleness of concrete. Hillerborg (1985) showed that maximum aggregate size affects the fracture energy ( $G_f$ ). The same results have been noticed by Nallathambi et al. (1985). While the results were not recognized by Petersson (1980) and Kleinschrodt and Winkler (1986), their results showed that the fracture energy is not affected by maximum aggregate size. Therefore, more investigations have been done by researchers to study the role of maximum aggregate size. Wolinski et al. (1987) reported that the crack surface of smaller aggregate (2-4 mm) is smoother than larger aggregate (8-32 mm) and there is no monotonic influence of aggregate size on fracture mechanics parameters. Similar results were also reported by Barr et al. (1986) for aggregate size from 5-20 mm. Regnault and Brühwiler (1990) investigated the fracture process zone of mortar ( $d_{max}= 3 \text{ mm}$ ) and concrete ( $d_{max}= 8 \text{ mm}$ ). They found that the size of aggregate affects both strain distribution and formation of microcracks, but the fracture process zone is more pronounced in concrete than mortar. Mihashi et al. (1991) showed that the fracture energy significantly increases when the aggregate size becomes larger; similarly the FPZ also gets wider. Besides, Mihashi and Nomura (1996) also reported that the length of the FPZ seems to be independent of the maximum aggregate size but the width is influenced by the maximum aggregate size. However, Tasdemir et al. (1999) found that fracture energy ( $G_f$ ) and characteristic length ( $l_{ch}$ ) increase as the aggregate size is increased. While Otsuka and Date (2000) showed that the width of the fracture core zone (FCZ) and the fracture process zone (FPZ) increase with the increase of the maximum aggregate size and the length of them shows an opposite trend. Issa et al. (2000a; 2000b) reported that the fracture energy and the fracture toughness increase with the increase of aggregate size and the fracture surface changes from smooth to rough and complex when aggregate size increases. Same trends were also obtained by Chen and Liu (2004) and Zhao et al. (2008) for high strength concrete. Wu et al. (2001) and Chen and Liu (2007) also used acoustic emission (AE) technique to investigate the effect of maximum aggregate size. Except obtaining the similar features for fracture surfaces, the results also indicated that the fracture energy and the total number of hits increased with the increase of the aggregate size. Thus, it can be summarized from the above discussion and literature review that fracture energy, fracture process zone and characteristic length increase as the aggregate size increases. The fracture properties are generally considered as size independent

properties. Therefore, aggregate size should have a direct relationship with size effect.

## 2. Relationship between the aggregate size and the size effect

The size effect on the failure is rigorously studied as the dependence of nominal strength ( $\sigma_N$ ) of geometrically similar structures on varying characteristic dimension ( $D$ ) when geometrically similar structures are compared. Due to distinctive fracture process in quasi-brittle materials, size effect is transitional between plasticity (strength based theories) and linear elastic fracture mechanics (LEFM). The transitional behaviour is caused by the fact that the fracture process zone (FPZ) size, equal to several inhomogeneity sizes (or max. aggregate size), is not negligible compared to the cross-sectional dimension of the member. It is well described by the [Bažant \(1984\)](#) and can be written as follows in the generalized form:

$$\sigma_N = \frac{Bf_t}{\sqrt{1 + \frac{D}{D_0}}} \quad (1)$$

where  $Bf_t$  and  $D_0$  are the empirical constants and are obtained by fitting the plots between the nominal strength ( $\sigma_N$ ) and size ( $D$ ) of geometrically similar specimens.

The above size effect law was obtained by the equivalence between the energy dissipation in a localised cracked zone and the energy stored due to applied load. In the size effect law (SEL), the parameter  $D_0$  was considered as the transitional structural dimension between the plasticity and LEFM [Bažant and Planas \(1998\)](#).  $D_0$  was related to the width ( $h_f$ ) and the relative length at the peak load ( $a_0/D$ ) of the energy dissipation zone as follows:

$$D_0 = \frac{h_f}{2k} \frac{D}{a_0} \quad (2)$$

where  $k$  is the slope of the energy dissipation zone.

[Equation \(1\)](#) was derived by simple energy release analysis. The SEL has also been derived by [Bažant and Kazemi \(1990\)](#) based on the simple asymptotic power scaling laws for very large and very small  $D$ , where [Equation \(1\)](#) will take the following form:

$$\sigma_N = \sqrt{\frac{E'G_f}{g(\alpha_0)D + g'(\alpha_0)c_f}} \quad (3)$$

where  $\alpha_0 = a_0/D$ ,  $g(\alpha_0)$  is the dimensionless energy release rate function of LEFM,  $g'(\alpha_0) = dg(\alpha_0)/d(\alpha_0)$ ,  $G_f$  is the fracture energy,  $E' = E/(1 - \nu^2)$  is the Young's Modulus for plane strain,  $\nu$  is Poisson ratio, and  $c_f$  is the effective length of the fracture process zone based on the equivalent elastic fracture mechanics. By setting [Equation \(3\)](#) as the form of classical [Equation \(1\)](#) one would get:

$$D_0 = c_f \frac{g'(\alpha_0)}{g(\alpha_0)} \quad (4)$$

and

$$Bf_t = \sqrt{\frac{E'G_f}{c_f g'(\alpha_0)}} \quad (5)$$

Similar to Equation (2), Equation (4) reveals that the transitional size  $D_0$  is directly proportional to the effective length of the FPZ. Recently it was confirmed by an experimental study that the size effect length parameters  $D_0$  and  $c_f$  are directly proportional to the aggregate size (Zhu et al. 2019). Material heterogeneity size or aggregate size thus plays an important role in the size effect on the mechanical and fracture behaviour of quasi-brittle materials like concrete.

### 3. A new size effect model taking into account heterogeneity size

Based on the discussion in Section 2 and recent experimental findings (Zhu et al. 2019), it can be reasonably assumed that:

$$D_0 = \gamma d_{max} \quad (6)$$

where  $\gamma$  is a material constant and is independent of the heterogeneity size or the structural size.

The size effect equation can now be written as:

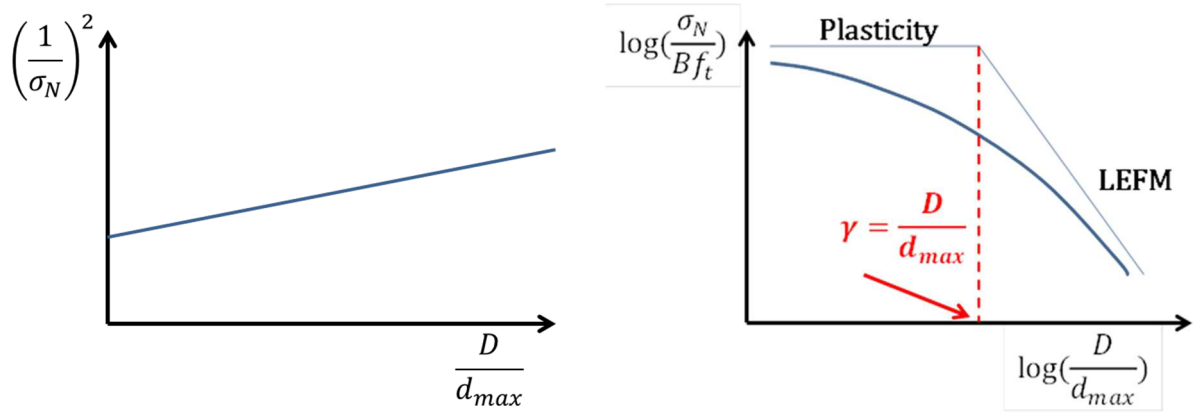
$$\sigma_N = \frac{Bf_t}{\sqrt{1 + \frac{D}{\gamma d_{max}}}} \quad (7)$$

The new form of size effect (Equation (7)) has many advantages over the classical form (Equation (1)). From the new size effect formulation one can predict the size effect based on true physical parameters, i.e. the ratio of the characteristic structural dimension to the maximum heterogeneity size ( $D/d_{max}$ ) instead of  $D/D_0$ .

The new size effect model can now be written in the form of linear equation in terms of  $1/(\sigma_N)^2$  and  $D/d_{max}$  as:

$$\frac{1}{(\sigma_N)^2} = \frac{1}{(Bf_t)^2} + \frac{1}{\gamma (Bf_t)^2} \frac{D}{d_{max}} \quad (8)$$

From the regression analysis, one can determine the constants  $Bf_t$  and  $\gamma$ . The regression analysis should be performed by varying the ratio  $D/d_{max}$  as shown in Figure 1(a). It can be done using the classical way by scaling  $D$  and keeping  $d_{max}$  constant. A new way proposed in this paper is to scale  $d_{max}$  and keep  $D$  constant. The size effect can be then illustrated on a non-dimensional plot as shown in Figure 1(b).



(a) (b)  
 Figure 1. Illustration of size effect curves using new size effect model  
 (a) regression curve (b) non-dimensional size effect plot.

In the new size effect model, the dimensionless material parameter  $\gamma$  is the ratio  $D/d_{max}$  at the transition between plasticity and LEFM. The behaviour of a structure will be close to LEFM (brittle behaviour) if its ratio  $D/d_{max}$  is larger than  $\gamma$ . However, the behaviour of the structure will be close to strength theory (ductile behaviour) if its ratio  $D/d_{max}$  is less than  $\gamma$ . Using this simple analysis, the design engineer will have more control on the size effect and can predict beforehand the behaviour of the structure with brittle or ductile behaviour for a specific structural dimension and the material microstructure.

#### 4. Experimental analysis using the new size effect approach

In this section a new approach is presented where the size effect is investigated by scaling material heterogeneity size and keeping the structural size the same. The material used was concrete, which is one of the widely used quasi-brittle materials. Three concretes were designed, where the aggregate size ( $d$ ) was scaled. In these concretes, the mortar content, water/cement ratio and all mix design parameters were kept as constant. While scaling the aggregate size ( $d$ ), complete grading curve was scaled with the same factor. Aggregate sizes were up-scaled in these concretes such that the volumetric fraction for each class of aggregate with respect to the maximum aggregate size, i.e.  $d(i)/d_{max}$  in each concrete remains the same and is equal to the reference grading curve. Section 4.1 explains the materials used in this study. Specimen details and loading setup are presented in Section 4.2. Section 4.3 is dedicated to present the experimental results of the size effect by using the new size effect model and scaling the heterogeneity size. In Section 4.4, the size effect is analysed by applying the classical approach, i.e. by scaling specimen size and using the new size effect model.

##### 4.1 Material properties and mix designs

Ordinary Portland cement CEM I 52.5N was used as a binder. Water-cement ratio (W/C) was maintained at 0.4 for all the mixes. Fine aggregate was crushed fine sand with the maximum size no greater than 2 mm. Coarse aggregate was crushed limestone. Three concrete mixes were designed, namely C05, C10 and C20, where the coarse aggregate size was varied. The maximum coarse aggregate size  $d_{max}$  was taken as 5.25 mm, 10.5 mm and 21 mm respectively. Table 1 shows the mixture proportions of the concretes. The three concrete mixes were designed so as to keep the same mortar volumetric proportion and properties.

Table 1. Mix proportions of concrete

Concrete	Unit Content ( $kg/m^3$ )					
	Water	Cement	Sand	Coarse aggregate		
				2 – 5.25 mm	4 – 10.5 mm	8 – 21 mm
C05	175	439	772	926		
C10	175	439	772	926		
C20	175	439	772	926		

In order to scale the complete grading curve, C10 concrete ( $d_{max} = 10.5 \text{ mm}$ ) was taken as the reference mix with the reference grading curve. The aggregate content was divided into twelve classes with respect to their size by using the ratio  $d(i)/d_{max}$ , as shown in Table 2, where  $d(i)$  is the aggregate size of the class and  $d_{max}$  is the maximum aggregate size in the complete grading curve.  $d_{max}$  was taken as 90% passing on the sieve analysis. The reference grading curve was then drawn by plotting the volumetric fraction against  $d(i)/d_{max}$  for each class. The next step was to obtain two aggregates mixes, one with  $d_{max} = 5.25 \text{ mm}$  (C05 concrete) and other with  $d_{max} = 21 \text{ mm}$  (C20 concrete). The availability of different classes of aggregates made it possible to achieve the reference grading curve for each aggregate mix.

Table 2. Coarse aggregate classes and volumetric fractions in each concrete mix

Class	$\frac{d(i)}{d_{max}}$	Volumetric fraction (%)		
		C05 $d_{max} = 5.25 \text{ mm}$	C05 $d_{max} = 10.5 \text{ mm}$	C05 $d_{max} = 21 \text{ mm}$
1	0.1	0.0	0.0	0.0
2	0.2	0.0	0.0	0.0
3	0.3	0.0	0.0	0.0
4	0.4	8.9	8.9	6.8
5	0.5	11.9	12.0	11.3
6	0.6	19.5	21.9	20.5
7	0.7	25.8	26.6	27.0
8	0.8	15.5	14.3	16.4
9	0.9	13.3	11.4	13.0
10	1.0	4.0	3.3	4.1
11	1.1	0.6	0.9	0.5
12	1.2	0.5	0.7	0.4

The volumetric fraction of each aggregate class was adjusted to achieve the closest match with the reference curve. Same volumetric fraction for each class in each aggregate mix shows that aggregate was scaled by considering the complete grading curve and keeping same volumetric fraction throughout the grading curve. Table 2 shows the aggregate classes and volumetric fractions for each mix. The final grading curve of each coarse aggregate mix is presented in Figure 2.



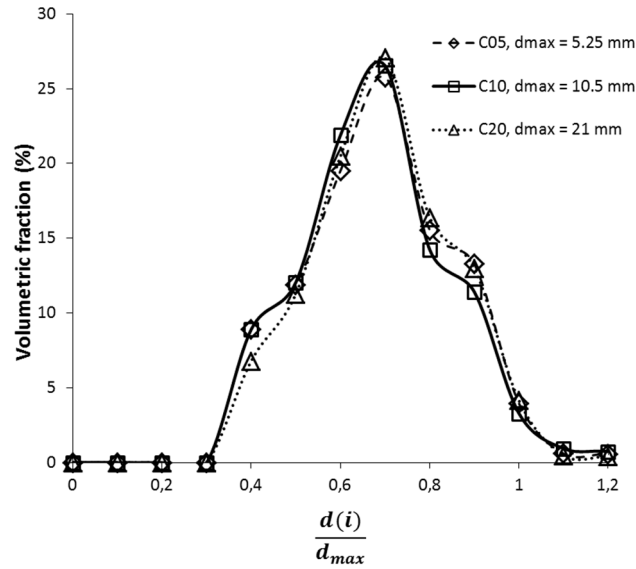


Figure 2. Coarse aggregate grading curves for individual concretes

## 4.2 Specimen preparation and testing procedure

Compression and Brazilian tests were carried out on  $\phi 110 \text{ mm} \times 220 \text{ mm}$  cylinders. Elastic modulus and compressive strength of the cylinders were measured according to ASTM C469 (ASTM 2010) and ASTM C39 (ASTM 2001), respectively. Three sets of LVDTs were used to measure the axial strains on the specimens. The static elastic modulus was defined as a chord modulus from the stress-strain curve with the first point at the strain level of 0.00005 and the second point at 40% of the maximum stress. The average mechanical properties and the corresponding standard deviations are given in Table 3.

Table 3. Mechanical properties of concrete mixes

Concrete	Brazilian Strength (MPa)	Compressive Strength (MPa)	Young's Modulus (GPa)
C05	$3.65 \pm 0.17$	$63.49 \pm 1.13$	$30.40 \pm 0.18$
C10	$3.81 \pm 0.32$	$72.97 \pm 1.03$	$31.90 \pm 0.66$
C20	$4.19 \pm 0.49$	$77.77 \pm 2.04$	$33.08 \pm 0.87$

Three-point bending tests were performed on the concrete specimens of  $100 \text{ mm} \times 100 \text{ mm} \times 400 \text{ mm}$  (width  $\times$  depth  $\times$  length). The beam was designed according to RILEM-TC 89 recommendation (RILEM 1990). Two specimens of each type were tested to consider the deviations of the results. The ratio of the vertical notch depth to the depth of beam was equal to 0.2 ( $a_0 = D/5$ ). The experimental setup is shown in Figure 3. In order to analyse the effect of specimen size, two more series of tests were conducted on the concrete specimens with the sizes of  $100 \text{ mm} \times 200 \text{ mm} \times 800 \text{ mm}$  and  $100 \text{ mm} \times 400 \text{ mm} \times 1600 \text{ mm}$ , respectively. The specimen sizes were designed so that the width ( $b$ ), the ratio of length to depth ( $L/D$ ) and the ratio of span to depth ( $S/D$ ) were maintained constant.



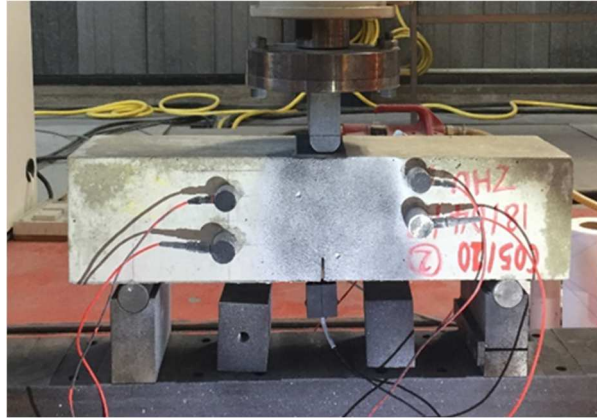


Figure 3. Experimental setup

The geometrical properties of the *D*-series concrete specimens are given in Table 4. It can be seen that new size effect analysis is performed on Series *D1*, *D2* and *D3* beams. In each series, concrete aggregate size was scaled, where  $d_{max}$  was varied as 5.25 mm, 10.5 mm and 21 mm. The heterogeneity size was scaled while keeping the beam size constant. The fracture tests employed a universal testing machine as per RILEM-TC 89 recommendation (RILEM 1990). Tests were conducted using a 160 kN servo-hydraulic machine under closed-loop crack mouth opening displacement (CMOD) control. Bending tests were performed with a controlled crack mouth opening displacement (CMOD) rate of 0.2  $\mu\text{m}/\text{sec}$  using a CMOD clip gauge. The load and CMOD were measured and recorded up to failure using a data acquisition system. For Series *D3*, only one beam was tested for each concrete. The obtained load-CMOD curves are presented in Figure 4 and show the characteristic quasi-brittle responses of the notched concrete beams.

Table 4. Geometric properties of *D*-series concrete specimens

Size Series	Concrete	$D$ (mm)	$b$ (mm)	$a_0/D$	$S/D$	$L/D$
<i>D1</i>	C05	100				
	C10	100	100	0.2	3.0	4.0
	C20	100				
<i>D2</i>	C05	200				
	C10	200	100	0.2	3.0	4.0
	C20	200				
<i>D3</i>	C05	400				
	C10	400	100	0.2	3.0	4.0
	C20	400				

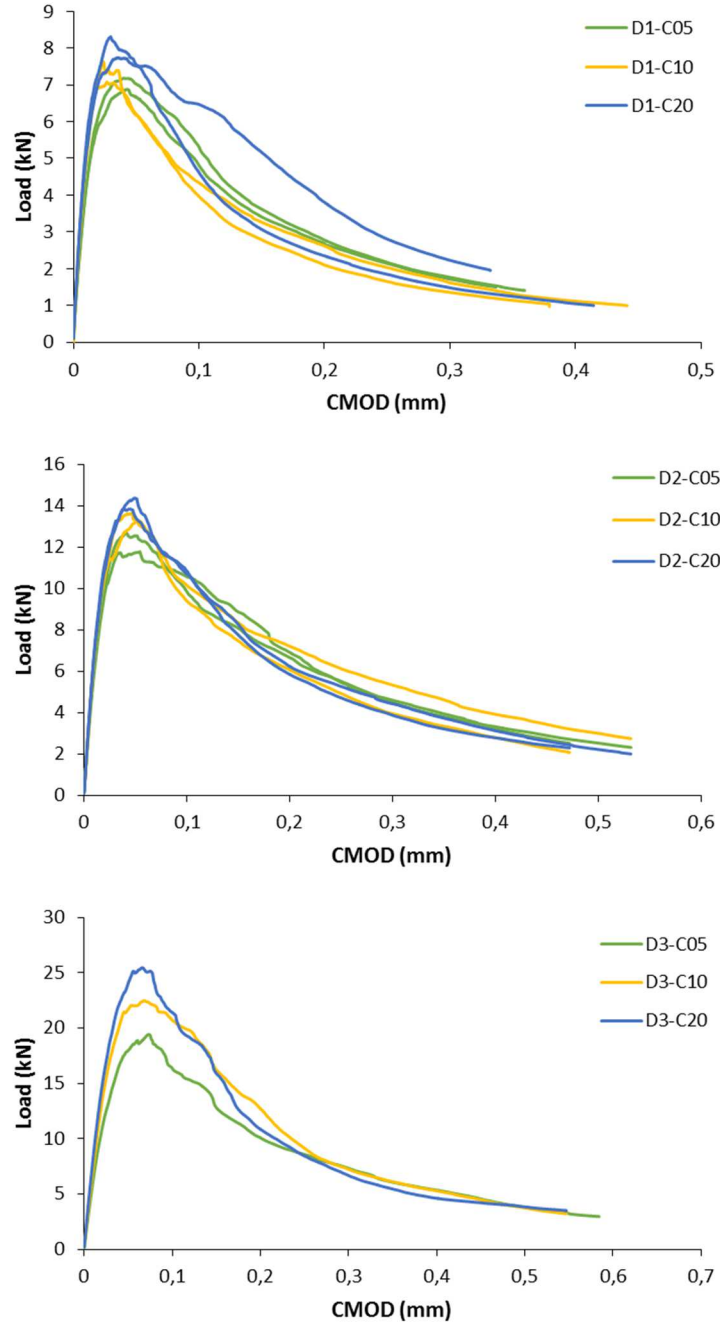


Figure 4. Load-CMOD curves from three-point bending tests on D1, D2 and D3 series.

### 4.3 Size effect analysis by scaling the heterogeneity size

The peak load is firstly corrected by considering the weight of beam as:

$$P_{max} = P_{max}^0 + \frac{2S + L}{2S} \cdot g_g \cdot m \quad (9)$$

where  $P_{max}$  is the corrected peak load,  $P_{max}^0$  is the peak load recorded by the load cell,  $m$  is the mass of specimen,  $S$  is the span,  $L$  is the specimen length, and  $g_g$  is the acceleration due to gravity.

The nominal strength is then calculated using the corrected ultimate load for each

specimen using the following equation:

$$\sigma_N = \frac{3 P_{max} S}{2bD^2} \quad (10)$$

According to the new size effect model Equation (7), linear regression between the nominal stress and  $D/d_{max}$  allows determining the coefficients  $Bf_t$  and  $\gamma$  in Equation (8) as follows:

$$Y = AX + C \quad (11)$$

$$X = D/d_{max}; Y = \left(\frac{1}{\sigma_N}\right)^2; \gamma = \frac{C}{A}; Bf_t = \frac{1}{\sqrt{C}} \quad (12)$$

Based on the concept of the equivalent elastic LEFM proposed by Bažant and Kazemi (1990) and Bažant and Planas (1998) and Equation (6), two major fracture parameters, the fracture energy ( $G_f$ ) and the effective length of process zone ( $c_f$ ), can be determined through:

$$G_f = \frac{(Bf_t)^2 \gamma d_{max} g(\alpha_0)}{\tilde{E}} \quad (13)$$

$$c_f = \frac{g(\alpha_0)}{g'(\alpha_0)} \cdot \gamma d_{max} \quad (14)$$

where  $\tilde{E} = E/(1 - \nu)$ ,  $E$  is the elastic modulus of concrete,  $\nu$  is the poisson ratio,  $g(\alpha_0)$  is the non-dimensional energy release rate, and  $g'(\alpha_0)$  is the derivative of  $g(\alpha_0)$  with respect to the relative initial crack length  $\alpha_0 = a_0/D$ .

The nominal stress for each beam is presented on the new size effect plot for each size series as shown in Figure 5. The results show a transitional behaviour for each concrete is well described by the new effect law curve. The parameters  $Bf_t$  and  $\gamma$  obtained for each size effect plot are given in Table 5. Both parameters  $Bf_t$  and  $\gamma$  are almost the same for all series, i.e. it is not affected by the specimen size or the aggregate size. From the size effect Equation (7),  $Bf_t$  is related to the strength of the structure when  $D/d_{max}$  approaches zero. The parameter  $\gamma$  is a new parameter introduced in the new size effect model Equation (7). This parameter is a physical quantity and is related to the brittleness of the material. It indicates the ratio  $D/d_{max}$  at the transition between plasticity and LEFM. Thus, the behaviour of quasi-brittle material is dependent on the ratio of the structural size to the heterogeneity size. The obtained values of  $Bf_t$  and  $\gamma$  from three series of tests indicate the validation of the approach and uniqueness of parameters irrespective of the specimen size and aggregate size used in the test.

It should be noticed that the size effect curve obtained for three series of tests is always the same. All the size effect plots in Figure 5 are transferred to those in Figure 6, where one can analyse the effect of the ratio of the specimen size to the aggregate size. It can be seen that with the decrease of the ratio, the behaviour of specimen approaches the hypothesis of strength criterion, and with the increase of the ratio, the behaviour approaches LEFM. This means that when the heterogeneity size in quasi-brittle materials like concrete is small enough compared to the structural size, the material behaviour becomes brittle and can be described

with fracture mechanics principles. It can be observed in Figure 6 that the specimens with the same  $D/d_{max}$  (the ratio irrespective of their aggregate size or specimen size) have always the same nominal strength and do not show any size effect. Thus, the size effect is caused by the relative increase of structural dimension with respect to the material heterogeneity size.

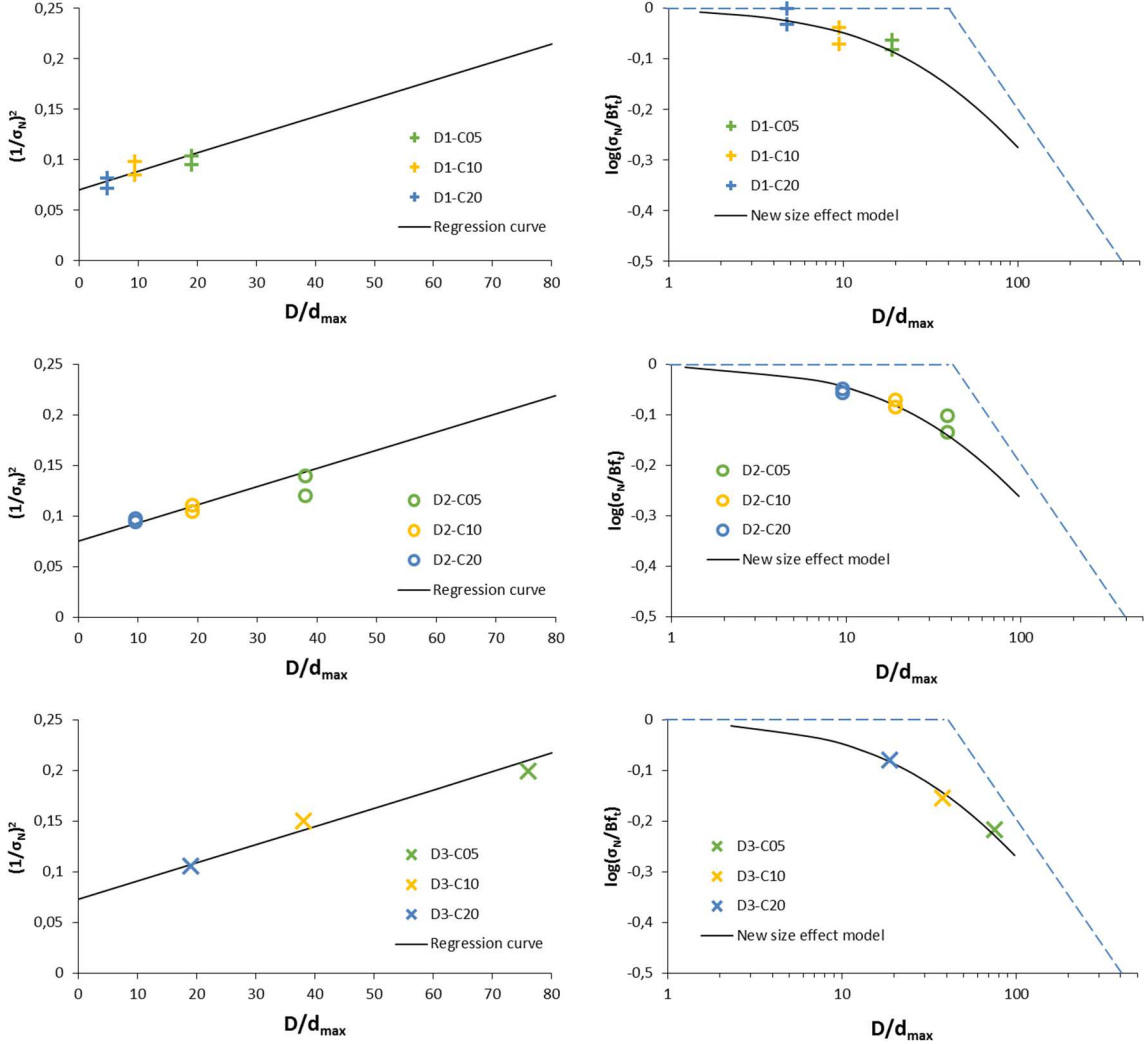


Figure 5. Size effect curves for D1, D2 and D3 series.

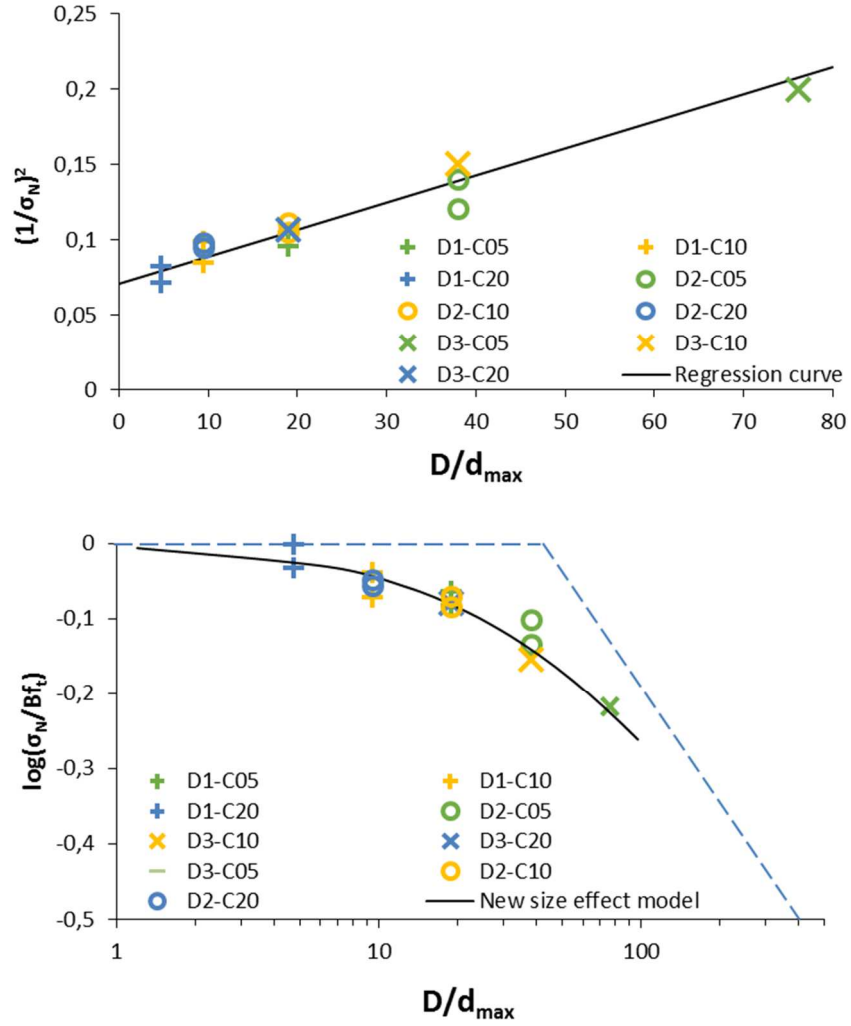


Figure 6. Combined size effect curves for D1, D2 and D3 series.

Table 5. Fracture properties from size effect analysis

Parameters	Size series			Average
	D1	D2	D3	
$\gamma$ (mm)	39	42	41	$40.7 \pm 1.5$
$Bf_t$ (MPa)	3.8	3.7	3.7	$3.73 \pm 0.1$

The fracture properties can now be determined by using Equations (13) and (14). One series of test is sufficient to determine the fracture properties of all three concretes. Three size series were used to determine the fracture energy and the results are presented in Table 6. It can be seen that the fracture energy obtained for a concrete does not depend on the specimen size used. Secondly, the fracture energy increases as the aggregate size increases, which is in accordance with the literature.

The effective length of the process zone ( $c_f$ ) can also be determined using Equation (14) for any concrete by using only the results for one size series. All three size series were used to determine  $c_f$  and the results are presented in Table 7. It can be seen that the  $c_f$  value obtained for a concrete does not depend on the specimen size used. Moreover,  $c_f$  increases as the aggregate size increases, which is also in accordance with the literature.

Table 6. Fracture energy ( $G_f$ ) from the new size effect law by scaling the heterogeneity size

Size series	$G_f$ of Concrete (N/m)		
	C05	C10	C20
D1	59	108	209
D2	57	109	209
D3	57	109	209
Average	57.7±1.1	108.7±0.6	209.0±0.0

Table 7. Effective length of the process zone ( $c_f$ ) from the new size effect law by scaling the heterogeneity size

Size series	$c_f$ of Concrete (mm)		
	C05	C10	C20
D1	74	148	297
D2	79	158	316
D3	77	154	308
Average	76.7±2.5	153.3±5.0	307.0±9.0

#### 4.4 Size effect analysis by scaling the specimen size

The advantage of the new size effect model is that one can analyse the size effect in a new way (scaling the heterogeneity size) or in the classical way by scaling the specimen size. The experimental tests carried out in this study make it possible to perform size effect analysis using any of these ways. The results of Series D1, D2 and D3 specimens allowed performing scaling of specimen size for each concrete.

The nominal stress for each concrete series (C05, C10 and C20) using geometrical similar specimens (D1, D2 and D3) is presented on the new size effect plot as shown in Figure 7. Similar to Bažant's size effect curve, the results show a transitional behaviour for each concrete and are well described by the new effect law curve. However, here the size is relative to the aggregate size ( $D/d_{max}$ ). The parameters of the new size effect law,  $Bf_t$  and  $\gamma$ , are obtained for each series and are given in Table 8. The parameters  $Bf_t$  and  $\gamma$  remain constant in all series. It should be noticed that the values are the same as obtained in the previous section by scaling the heterogeneity size. Thus scaling the heterogeneity size or the specimen size gives the same size effect. It is the ratio of the specimen size to the heterogeneity size which yields the size effect.

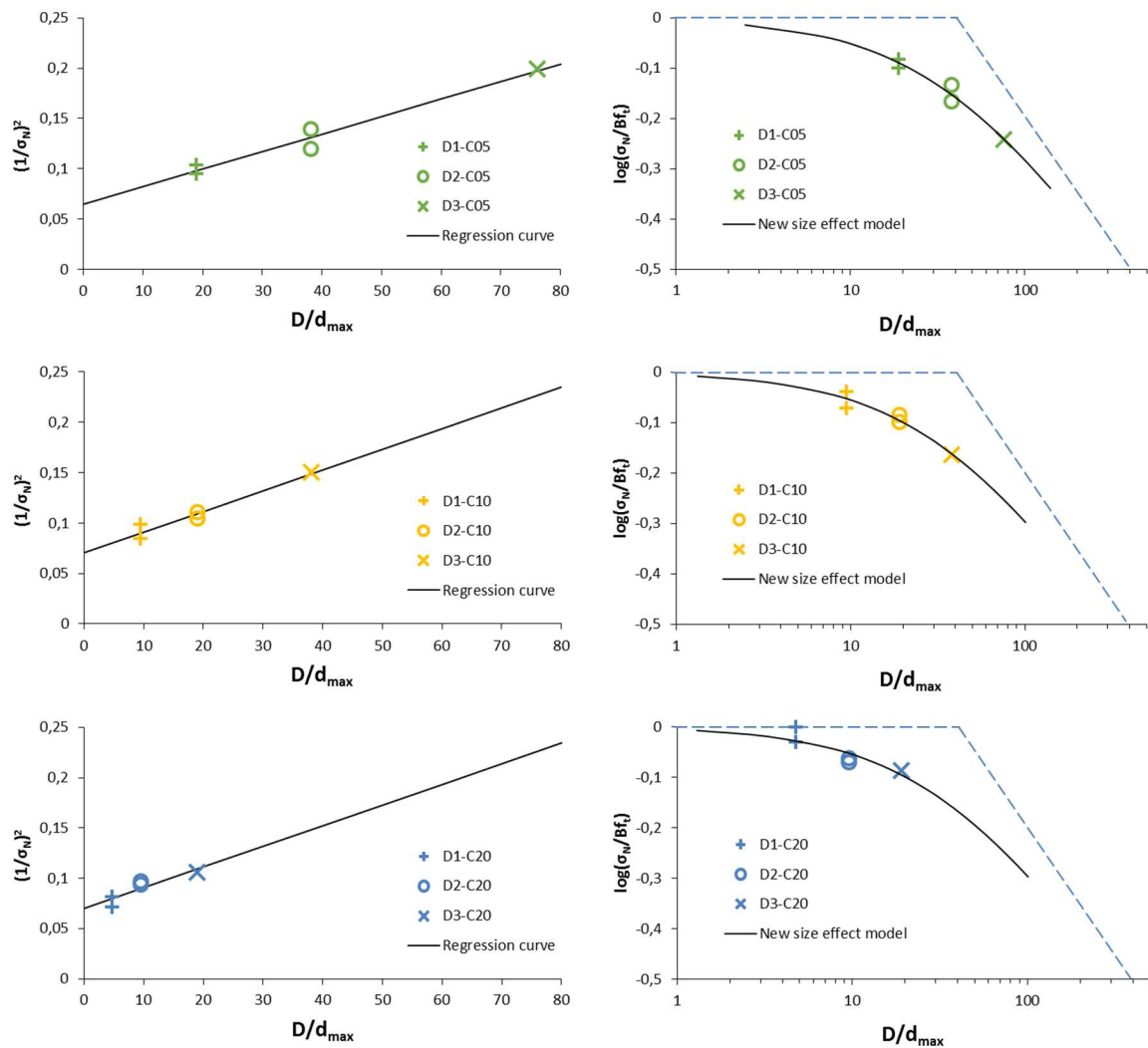


Figure 7. Size effect curves for C05, C10 and C20 series.

Table 8. Fracture properties from size effect analysis

Parameters	Concrete			Average
	C05	C10	C20	
$\gamma$ (mm)	37	34	34	$35.0 \pm 1.7$
$Bf_t$ (MPa)	3.9	3.8	3.8	$3.8 \pm 0.06$

It should be noticed that the size effect curves obtained for all concrete series are identical as shown in Figure 7. All the size effect curves are then converted to one single curve as shown in Figure 8, where one can analyse the effect of ratio between the specimen size and the aggregate size irrespective of the type of concrete. It can be seen that Figure 8 by scaling the specimen size is exactly the same as Figure 6 by scaling the heterogeneity size. This means that with the new size effect law Equation (7), the scaling of the heterogeneity size or the specimen size produces the same size effect curve.



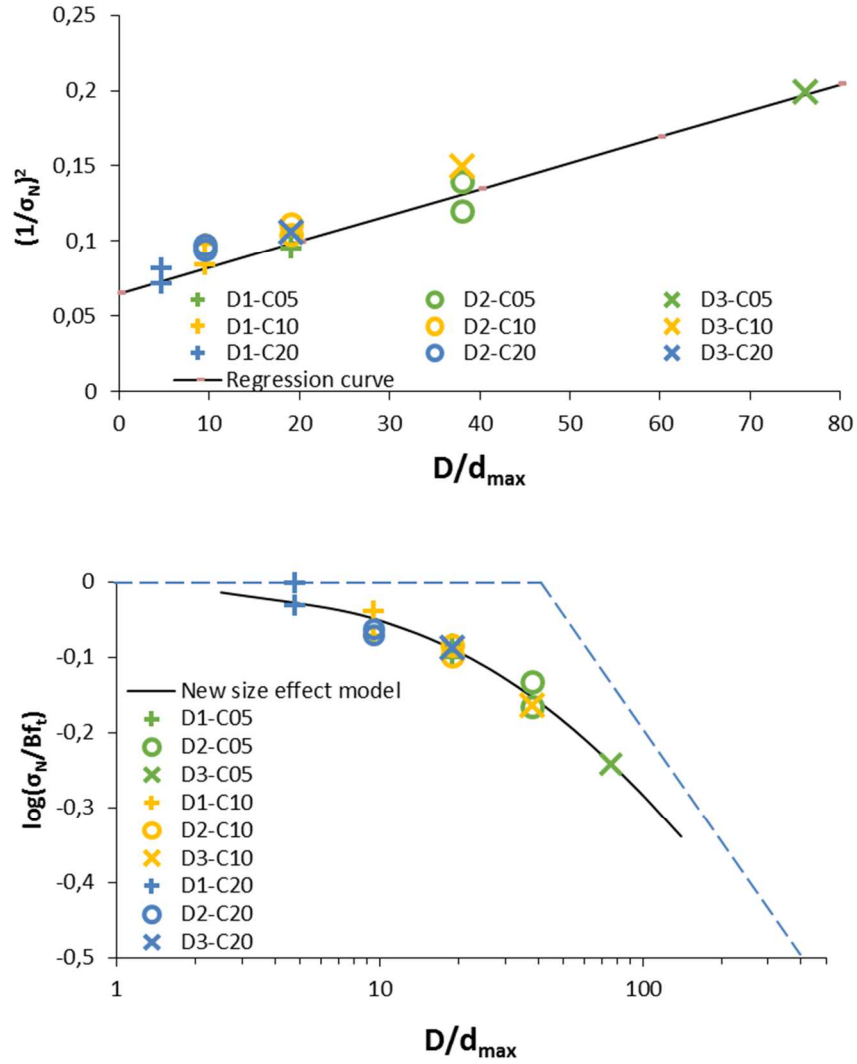


Figure 8. Combined size effect curves for C05, C10 and C20 concrete.

The fracture properties obtained from scaling the specimen size can now be determined by using Equations (13) and (14). One concrete series of test is sufficient to determine fracture properties of any concrete where the aggregate size is scaled. However, in this study, all three concrete series were used to determine fracture parameters and the results are presented in Table 9. It can be seen that the fracture energy obtained for a concrete does not depend on the specimen size used. Secondly, the fracture energy increases as the aggregate size increases, which is in accordance with the literature.

Table 9. Fracture energy ( $G_f$ ) from the new size effect approach by scaling the specimen size

Size effect series	$G_f$ of Concrete (N/m)		
	C05	C10	C20
C05	58	111	215
C10	50	95	183
C20	50	95	183
Average	$52.7 \pm 4.6$	$100.3 \pm 9.2$	$193.7 \pm 18.5$

The effective length of process zone ( $c_f$ ) can also be determined using Equation (14) for any concrete by using only one size series results. All three size series were used to determine

$c_f$  and the results are presented in Table 10. It can be seen that  $c_f$  obtained for a concrete does not depend on the specimen size used. Moreover,  $c_f$  increases as the aggregate size increase, which is in accordance with the literature.

Table 10. Effective length of the process zone ( $c_f$ ) from the new size effect approach by scaling the specimen size

Size effect series	$c_f$ of Concrete (mm)		
	C05	C10	C20
C05	71	141	283
C10	65	130	261
C20	77	154	308
Average	71.0±6.0	142.0±12.0	284.0±23.5

## 5. Conclusions

The paper presents a new approach to investigate the size effect on the failure of quasi-brittle materials like concrete. In these materials, the heterogeneity size plays an important role in the mechanical responses and failure modes of structures. The main conclusions are given below:

- A new size effect model is presented where the heterogeneity size is taken into account while scaling the structural size. The new model investigates the size effect by using the ratio of the structural size to the heterogeneity size ( $D/d_{max}$ ) as the cause of the size effect but not the structural size  $D$  alone. The new size effect model is an improved version of Bažant's size effect law by directly taking into account the effect of the heterogeneity size in the size effect.
- The proposed size effect model introduces a new parameter  $\gamma$ , which is the ratio  $D/d_{max}$  at the transition from plasticity and LEFM. This parameter is a physical quantity which enables to easily predict the brittleness of a structure.
- Section 4 of this paper presents a new experimental approach, where the size effect is investigated by scaling the heterogeneity size ( $d_{max}$ ) and keeping the structural size ( $D$ ) constant. The scaling of the heterogeneity size (the aggregate size here) is performed by taking into account complete gradation of the aggregate content. The complete grading curve is scaled at the same time with the same scaling factor and the constant volumetric ratio for each class aggregate class.
- The down-scaling of the aggregate size and keeping the specimen size constant, i.e. increasing the ratio  $D/d_{max}$ , shows the decrease in the nominal strength. The size effect is transitional between two asymptotes i.e. plasticity and LEFM.
- The size effect obtained by the new approach, i.e. down-scaling of the aggregate size and keeping the specimen size constant, shows similar behaviour to the classical size effect approach by up-scaling the specimen size and keeping the aggregate size constant. The two approaches yield the same fracture energy and effective length of fracture process zone. However, the new approach is much easier to perform experimentally or numerically as it includes only one size.
- The common size effect observed on the strength of the structure is a function of both the structure size and heterogeneity size. It is the ratio between the two quantities which imparts the overall size effect.
- $G_f$  and  $c_f$  have been estimated through various ways (i) by scaling the heterogeneity size for various size series (Tables 6 and 7 respectively) and (ii) by scaling the specimen size for various concrete series (Tables 9 and 10 respectively). For same

heterogeneity size, the values  $G_f$  and  $c_f$  are almost same and thus independent of structural size  $D$  or the ratio  $D/d_{max}$ . The comparison of these quantities with equivalent LEFM analysis would be an interesting task but is not covered in the scope of this paper.

- The new size effect law provides the relationship between heterogeneity size and structural size. It is validated on a broad range of  $D/d_{max}$  and also the most commonly used  $D/d_{max}$  in the studies on concrete fracture. The new size effect law (Equation (7)) becomes analogous to Bažant's size effect law if only structural size is scaled and therefore has the same limitations e.g. approximate estimation of  $\sigma_N$  when  $D \rightarrow 0$  (Bažant 1997; Morel and Dourado 2011).
- Two specimens of each type of beam were tested to validate the approach. Only one specimen for large beam was tested. More tests will be conducted in the next studies to further validate the new size effect formulation

## References

Aïtcin PC, Mehta PK. Effect of coarse aggregate characteristics on mechanical properties of high-strength concrete. *Materials Journal* 1990; 87(2):103-107.

Alam SY, Saliba J, Loukili A. Fracture examination in concrete through combined digital image correlation and acoustic emission techniques. *Construction and Building Materials* 2014; 69:232-242.

ASTM C469, Standard Test Method for Static Modulus of Elasticity and Poisson's Ratio of Concrete in Compression, in *Annual Book of ASTM Standards*, ed. Philadelphia: American Society of Testing and Materials, 2010, pp. 255-258.

ASTM C39, Standard Test Method for Compressive Strength of Cylindrical Concrete Specimens, in *Annual Book of ASTM Standards*, ed. Philadelphia: American Society of Testing and Materials, 2001.

Barr B, Hasso E, Weiss V. Effect of specimen and aggregate sizes upon the fracture characteristics of concrete. *International Journal of Cement Composites and Lightweight Concrete* 1986; 8(2):109-119.

Bažant ZP. Size effect in blunt fracture: concrete, rock, metal. *Journal of Engineering Mechanics* 1984; 110(4):518-535.

Bažant ZP. Scaling of quasibrittle fracture: asymptotic analysis. *International Journal of Fracture* 1997; 83:19-40.

Bažant ZP, Kazemi MT. Determination of fracture energy, process zone length and brittleness number from size effect, with application to rock and concrete. *International Journal of Fracture* 1990; 44(2):111-131.

Bažant ZP, Planas J. *Fracture and Size Effect in Concrete and Other Quasibrittle Materials*. Boca Raton: CRC press, 1998.

Chen B, Liu JY. Effect of aggregate on the fracture behavior of high strength concrete. *Construction and Building Materials* 2004; 18(8):585-590.

Chen B, Liu J. Investigation of effects of aggregate size on the fracture behavior of high performance concrete by acoustic emission. *Construction and Building Materials* 2007; 21(8):1696-1701.

Goble CF, Cohen MD. Influence of aggregate surface area on mechanical properties of mortar. *ACI Materials Journal* 1999; 96(6):657-662.

Hillerborg A. Results of three comparative test series for determining the fracture energy  $G_F$  of concrete. *Materials and Structures* 1985; 18(5):407-413.

Issa MA, Issa MA, Islam MS, Chudnovsky A. Size effects in concrete fracture – Part I Experimental setup and observations. *International Journal of Fracture* 2000; 102(1):1-24.

Issa MA, Issa MA, Islam MS, Chudnovsky A. Size effects in concrete fracture – Part II Analysis of test results. *International Journal of Fracture* 2000; 102(1):25-42.

Kleinschrodt H, Winkler H. The influence of the maximum aggregate size and the size of specimen on fracture mechanics parameters. *Fracture Toughness and Fracture Energy of Concrete*. Ed. Wittmann FH, Elsevier Science Publisher Amsterdam 1986; pp. 391-402.

Morel S, Dourado N. Size effect in quasibrittle failure: Analytical model and numerical simulations using cohesive zone model. *International Journal of Solids and Structures* 2011; 48(10):1403-1412.

Mihashi H, Nomura N, Niiseki S. Influence of aggregate size on fracture process zone of concrete detected with three dimensional acoustic emission technique. *Cement and Concrete Research* 1991; 21(5):737-744.

Mihashi H, Nomura N. Correlation between characteristics of fracture process zone and tension-softening properties of concrete. *Nuclear Engineering and Design* 1996; 165(3):359-376.

Nallathambi P, Karihaloo BL, BS Heaton. Various size effects in fracture of concrete. *Cement and Concrete Research* 1985; 15:117-126.

Neville AM. *Properties of Concrete*. Pearson, Harlow, England; New York, NY, U.S., 2011.

Otsuka K, Date H. Fracture process zone in concrete tension specimen. *Engineering Fracture Mechanics* 2000; 65(2):111-131.

Petersson P. Fracture energy of concrete: practical performance and experimental results. *Cement and Concrete Research* 1980; 10(1):91-101.

Regnault P, Brühwiler E. Holographic interferometry for the determination of fracture process zone in concrete. *Engineering Fracture Mechanics* 1990; 35(1-3):29-38.

RILEM Recommendation. *Fracture Mechanics of Concrete – Test Methods, Size effect method for determining fracture energy and process zone size of concrete*. *Materials and Structures* 1990; 23:461-465.

Tasdemir C, Tasdemir MA, Mills N, Barr BI, Lydon FD. Combined effects of silica fume, aggregate type, and size on post-peak response of concrete in bending. *ACI Materials Journal* 1999; 96(1):74-83.

Weibull W. *A Statistical Theory of the Strength of Materials*. Royal Swedish Institute for Engineering Research 1939.

Wolinski S, Hordijk DA, Reinhardt HW, Cornelissen HA. Influence of aggregate size on fracture mechanics parameters of concrete. *International Journal of Cement Composites and Lightweight Concrete* 1987; 9(2):95-103.

Wu K, Chen B, Yao W. Study of the influence of aggregate size distribution on mechanical properties of concrete by acoustic emission technique. *Cement and Concrete Research* 2001; 31(6):919-923.

Zhao Z, Kwon SH, Shah SP. Effect of specimen size on fracture energy and softening curve of concrete – Part I Experiments and fracture energy. *Cement and Concrete Research* 2008; 38(8):1049-1060.

Zhu R, Alam SY, Loukili A. An experimental investigation of the correlation between aggregate size effect and structural size effect on concrete failure. *Engineering Fracture Mechanics* 2019 (under review).